Available online at www.sciencedirect.com

ScienceDirect

Ceramics International 39 (2013) 9263–9272

CERAMICS INTERNATIONAL

www.elsevier.com/locate/ceramint

Effect of zirconia on ablation mechanism of asbestos fiber/phenolic composites in oxyacetylene torch environment

Mir Asad Mirzapour[a,*], Hasan Rezaei Haghighat[a], Zahra Eslami[b]

[a]Engineering Research Institute, P.O. Box: 13445-754, Tehran, Iran
[b]Department of Chemical Engineering, Amirkabir University of Technology, P.O. Box: 15875-4413, Tehran, Iran

Received 18 April 2013; received in revised form 9 May 2013; accepted 9 May 2013
Available online 30 May 2013

Abstract

Micron-size zirconium oxide (ZrO_2) was used to improve the thermal stability and ablation properties of asbestos fiber/phenolic composites and to reduce their final cost. ZrO_2/asbestos/phenolic composites were prepared in an autoclave by the curing cycle process. The densities of the composites were in the range of 1.64–1.82 g/cm^3. The ablation properties of composites were determined by oxyacetylene torch environment and burn-through time, erosion rates and back surface temperature in the first required 20 s. To understand the ablation mechanism, the morphology and phase composition of the composites were studied by scanning electron microscopy, energy dispersive spectroscopy and X-ray diffraction. Thermal stability of the produced materials was estimated by means of thermal gravimetric analysis, in air which consisted of dynamic scans at a heating rate of 10 °C/min from 30 to 1000 °C with bulk samples of about 23 ± 2 mg. The thermal stability of the composites was enhanced by adding ZrO_2. The results showed that the linear and mass ablation rates of the composites after adding 14 wt% ZrO_2 decreased by 58% and 92%, respectively. The back surface temperature of a sample with 14% zirconia was 49% lower than that of pure composite. The SEM studies showed that, modified composites displayed much lower porosity than that of non-modified composite and the destruction of asbestos fibers was very low. On the other hand, it appeared that a thin melted layer of ZrO_2 covered the surfaces of zirconia-containing composites.

Keywords: Phenolic composite; Thermal stability; Linear ablation rate; Back surface temperature

1. Introduction

Thermal protection systems (TPS) are vital to the integrity of systems subjected to severe heating environments, such as hypersonic entry/re-entry vehicles, rocket engine nozzles, and heat shield and rocket combustion chambers. In particular, the use of a TPS to protect the payload of a hypersonic or planetary exploration vehicle from extremely high aerothermal heating rates display severe challenges due to TPS mass constraints. For very intense aerothermal heating environments, ablative TPS systems so far represent the only viable and fail-safe option. Ablative systems operate by absorbing heat through thermal decomposition and rejecting it via pyrolysis gas injection back into the boundary layer gas and re-radiation [1–3]. Ablative materials have been the subjects of many experimental and numerical studies, particularly in the 1960s and 1970s [4,5].

Most ablative TPS materials are reinforced composites where organic resins are used as matrices. When heated, the resin pyrolysis generates gaseous products (mostly hydrocarbons) that permeate through a solid and diffuse toward the external heated surface and proceed into the boundary layer, where the heat transfer processes take place. The resin pyrolysis also produces a carbonaceous residue, termed as char. The process is typically endothermic and pyrolysis gases are heated as they percolate toward the surface, thus transferring energy from the bulk of the composite into the pyrolysis gas.

The entering of the pyrolysis gases into the boundary layer alters its properties, generally resulting in reduction of convective heating. However, the gases may undergo chemical reactions with the boundary layer gases, thus influencing the net heat transferred into the surface. Furthermore, chemical

*Corresponding author. Tel.: +98 26 36636904, +98 9198098785; fax: +98 21 66284824.
E-mail addresses: faribamirzapour1@gmail.com, aidinmirzapour@yahoo.com (M.A. Mirzapour).

0272-8842/$ - see front matter © 2013 Elsevier Ltd and Techna Group S.r.l. All rights reserved.
http://dx.doi.org/10.1016/j.ceramint.2013.05.034

reactions can result in consumption of the surface material leading to surface recession. Reactions can be endothermic (vaporization or/and sublimation) or exothermic (oxidation) and will have an important impact on net energy to the surface. Clearly, in comparison to reusable TPS, the interaction of ablative TPS materials with the surrounding gases is much more complex as more numerous mechanisms are involved to accommodate the intense heating [6–8]. Due to the very high temperature attained on the surface of the TPS, several events can occur [9,10]:

1. Re-radiation of thermal energy from the outer surface into the atmosphere. At equilibrium temperature the entire incoming energy is dissipated;
2. pyrolysis taking place in the outer layer;
3. outer layers are charred and the pyrolysis zone advances toward inner layers;
4. soft char is removal from the surface by aerodynamic shear force (mechanical ablation).

The TPS, first developed in the early stages of space exploration, is today still widely investigated and advanced studies are driven by a strong request in terms of high heat flux resistance and cost effectiveness.

However, with the development of new aerospace vehicles, the comprehensive properties of the currently used ablatives cannot meet all the commercial and military demands. Therefore, ablative composites need to be infiltrated with refractory materials such as metals and carbides/borides to modify the ablative materials. Recently, different kinds of fillers, such as boron nitride, aluminum nitride, silicon nitride, alumina, silicon carbide, silica and diamond have been studied to improve the thermal behavior of polymer composites [11–14]. Lombardi et al. have investigated the role of layered fillers and equiaxial filler on ablative properties of composites based on PPO blend [15,16]. Some extensive research works have been carried out on the effect of zirconium carbide on microstructure and ablation properties of composites [17–22]. Erica et al. have improved ablation resistance of C/C composites using ZrB_2 and B_4C [23]. Various studies have been carried out to improve the thermal stability and ablation properties of asbestos/phenolic composite using nanosilicate by Bahramian et al. [24–27].

The interest in ZrO_2 as a refractory material is due to its thermo-physical properties such as low thermal expansion, low thermal conductivity, simple process ability, and low cost [28]. To the best of our knowledge, few works have been conducted on the thermal stability, microstructure and ablation properties of composites containing ZrO_2 additive. Chen et al. have investigated the effect of ZrO_2 powders on the pyrolysis of polycabosilanes coating under laser ablation [29]. Recently, Srikanth et al. have studied the mechanical, thermal and ablative properties of zirconia, carbon nanotube modified carbon/phenolic composites [30]. Effect of ZrO_2 on ablation properties of carbon fiber and ceramic fiber composites was studied in our previous paper [31]. In the present work, effect of ZrO_2 on the thermal stability, microstructure and ablation properties of a mineral fiber (asbestos) reinforced composite is investigated.

2. Experimental

2.1. Material preparation

Resole-type phenolic resin (IL800/2, Resitan Company) was used as matrix precursor of composites. The resin had a solid content of around 81% and a carbon yield of about 63% at 1000 °C in nitrogen atmosphere and density 1.1 g/cm^3. The viscosity of liquid resin at 20 °C was 600–800 mPa.s. Plain weave asbestos (chrysotile-type) fiber cloth (grade AAA; 1100 g/m^2) was used as reinforcement for phenolic composites. The fiber density was 2.1 g/cm^3. ZrO_2 powder (Hetian Ceramic Company) with an average particle size of about 7 μm and purity $>95\%$ was used as refractory filler.

2.2. Asbestos/ZrO_2/phenolic prepregs preparation

The fabrication of composite, arranged in 3 layers of plain weave asbestos fiber cloth, included the manual impregnation (hand lay-up method) with phenolic resin, previously mixed with ZrO_2 in the proportion of 0%, 7%, 10.5%, 14%, 17.5% and 21% based on resin weight. Each layer was put upon the previous layer in the same orientation and impregnated to complete the sequence of 3 layers. The impregnated fabrics were left in the prepregging rack at ambient temperature for 24 h to evaporate the solvent inside for better impregnation of the resin into fabrics.

2.3. Asbestos/ZrO_2/phenolic composites fabrication

Asbestos/ZrO_2/phenolic composites were fabricated in an autoclave by a conventional vacuum bagging method. Fig. 1 represents a cure profile of temperature, time and pressure to fabricate the composite in this work. After curing, the composites were post-cured for 2 h at 180 °C. The as-produced composites were designated as CZW-*y*, in which *y* indicated the mass content (wt%) of ZrO_2 in asbestos/phenolic composites. The apparent density (overall mass-to-

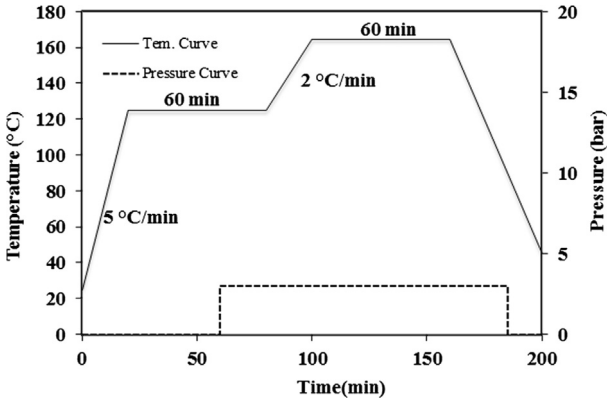

Fig. 1. A cure profile for fabrication of composite.

Table 1
Density and porosity of the samples.

Samples	Content of ZrO_2 (wt%)	Sample density (g/cm^3)	Porosity (%)
CZW-0	0	1.64	4.6
CZW-7	7	1.68	4.7
CZW-10.5	10.5	1.75	4.5
CZW-14	14	1.77	4.3
CZW-17.5	17.5	1.80	5.1
CZW-21	21	1.82	4.9

volume ratio) and porosity of the samples are listed in Table 1. The obtained composite was 40 × 40 cm in size. The thickness was 4 mm. All the composites were cut into a large number of required size specimens for the experimental purpose.

2.4. Mechanical tests

To study the mechanical properties of the composites, 3-points bending test was performed on an electronic universal testing machine (H&P 50, Germany). The load velocity was 1 mm/min. The effective size of the samples was 11.5 mm × 20 mm × 4 mm. The number of specimens used in the bending test was 6.

2.5. Thermal stability tests

Thermogravimetric analysis (TGA) was carried out in an air atmosphere, using rectangular test specimens with each estimated weight of 23 ± 2 mg, heating up 1000 °C, under a constant flow of dry air with heating rate of 10 °C/min. The oxidation behavior of the composite, as well as of its individual components, was evaluated by the weight loss method in a Lin Feif PT-100 thermogravimetric analyzer.

2.6. Ablation experiment

The appropriate testing of ablative materials required the use of hyperthermal environments with very high heat fluxes. This device was able to produce both the high temperature flame (up to 3000 °C) and the high heat flux. It is noteworthy to mention that the measurements were carried out with an oxyacetylene torch performed in an oxidative environment, i.e., under the conditions in which the degradation processes of the samples were maximized by their interactions with oxygen.

The ablation test was performed using an oxyacetylene flame torch and the characteristic values were calculated based on ASTM E285-80. Plate test specimens were of 80 mm × 80 mm in size and 40 mm in thickness. K-tape thermocouple was firmly attached with epoxy resin at the center of back faces of a specimen to record temperature changes as a function of time during the test. The external body of the thermocouples was protected using two alumina tubes. The distance and the angle between the specimen surface and the torch tip were 20 mm and 90°, respectively. The flame temperature in the present ablation testing system was estimated to be approximately 3000 °C and the heat flux was about 80 kW/m^2.

The ablation test was steadily conducted until the specimen was burnt through. Both the linear and mass ablation rates were calculated by dividing the specimen thickness or the weight change before and after the test into a burn-through time for each specimen. The average value was taken from the result after repeating the five specimens.

2.7. Characterization

The widest and most effective way of evaluating the erosion rate of an ablative material subjected to a hyperthermal environment is based on an analysis of the post-test specimen surfaces by optical and scanning electron microscopy (SEM). This analysis was performed both on the pristine and on the burnt samples, allowing the study of the initial morphology of the composites and of the effects of the high-temperature exposure. This analysis was accomplished by SEM combined with energy dispersive spectroscopy (EDS) in a VEGA2/TESCAN. To reduce electron charging, the samples were sputter coated with gold. The phases of composites were analyzed by X-ray diffractometer (XRD) with Cu-Kα radiation. Data were digitally recorded in a continuous scan mode in the angle (2θ) range of 5–85° with a scanning rate of 1 °/s.

3. Results and discussion

3.1. Morphological characterization

The morphology of the produced materials was investigated by means of a SEM analysis. Fig. 2a and b refers to the fractured surface of the CZW-0. These SEM images show the typical bundles of long chrysotile fibers. Fig. 2c and d shows some representative pictures of the CZW-14. By increasing the magnification, it is possible to clearly identify the ZrO_2 particles (a rectangular structure) and chrysotile fibers embedded in the phenolic matrix.

3.2. Thermal stability

Fig. 3 compares the TGA curves of neat resin and as-received composites. This figure shows that the thermal decomposition of the modified composites (CZW-0) shifts toward higher temperature range compared with that of pure composite, and confirms the enhancement of thermal stability of the composites. Evidently, it shows that major weight losses are observed within the range of ~380–800 °C for all the specimens.

3.3. Mechanical and ablation properties

The mechanical properties of as-received composites are listed in Table 2. It can be seen that the strength and modulus of bending of the as-received composites increase by increase in ZrO2 content (≤14.4 wt%), but they decrease when the content of ZrO_2 is ≥17.5 wt% for CZW-17.5.

The ablation properties of composites are shown in Table 2. A similar tendency in drop in ablation rates is found in samples

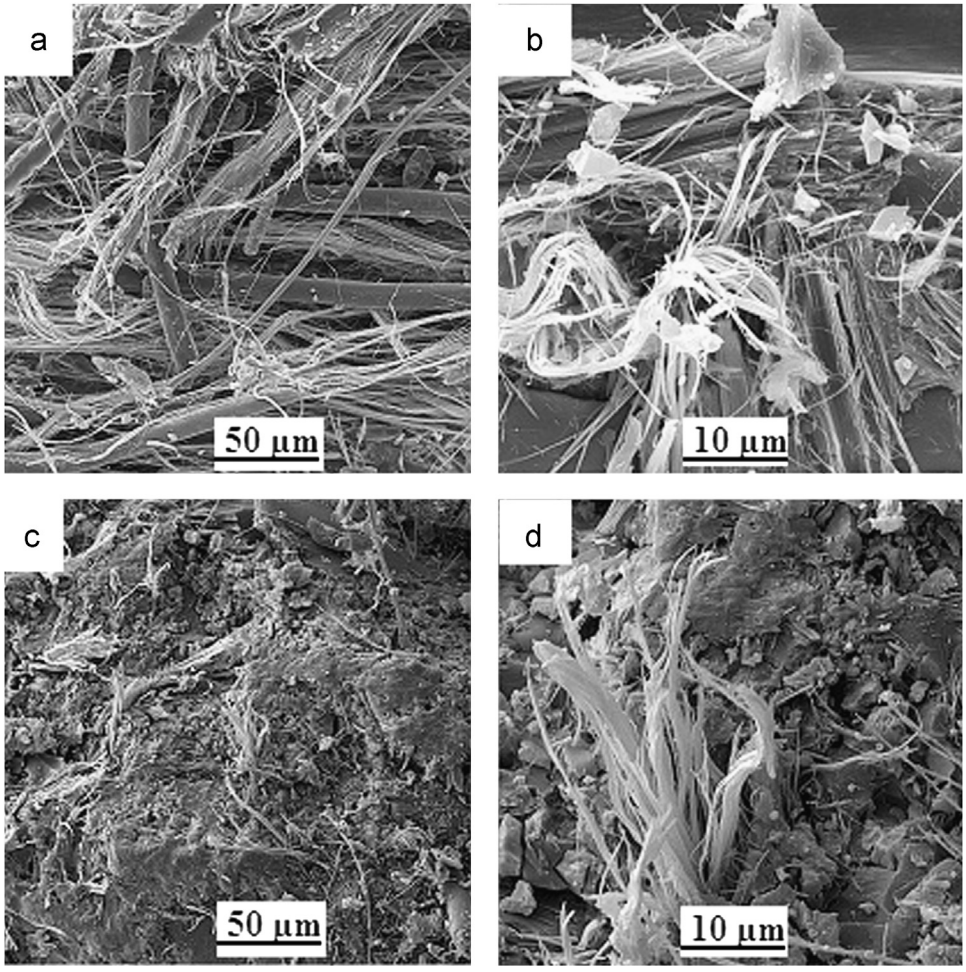

Fig. 2. SEM images of the fractured surfaces of composites: (a) and (b) CZW-0, and (c) and (d) CZW-14.

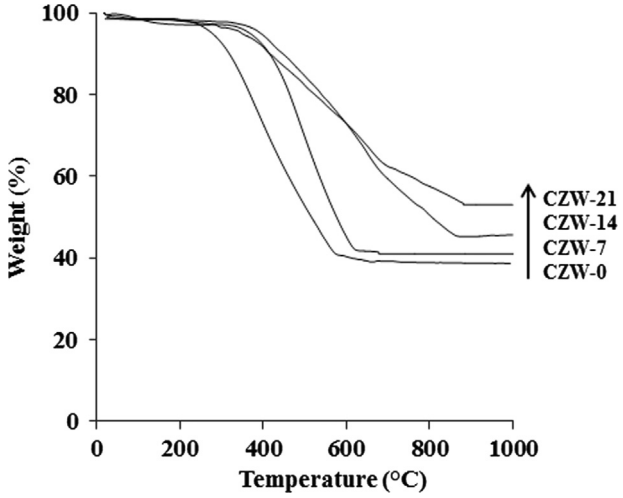

Fig. 3. The TGA thermogram of weight loss for CZW-0, CZW-7, CZW-14 and CZW-21.

with increased ZrO_2 content. At the beginning, the linear and mass ablation rates of the unmodified composite are 0.538 mm/s and 0.146 g/s, respectively. Then, they decrease rapidly when the ZrO_2 content is below 10.5 wt%, followed by a slow drop when the ZrO_2 content is less than 17.5 wt%, and finally remains more or less constant at higher ZrO_2 content. The linear and mass ablation rates of CZW-14% are 0.340 mm/s and 0.076 g/s, respectively. The linear and mass ablation rates of unmodified composites are dropped by about 58% and 92%, respectively by addition of 14% zirconia. Compared with montmorillonite/phenolic/asbestos ablative nanocomposites (highly filled polymer-layered silicate nanocomposites as a new class of ablative materials) which had displayed a linear ablation rate of 0.155 [32], the zirconia/phenolic/asbestos in our findings showed highly improved ablation resistance.

Table 2
Mechanical and ablation properties of ZrO_2-filled asbestos composites and pure asbestos composites.

Samples	Bending strength (MPa)	Modulus of bending (GPa)	Linear ablation rate (mm/s)	Mass ablation rate (g/s)
CZW-0	59.51	5.3	0.146	0.538
CZW-7	73.90	5.8	0.084	0.368
CZW-10.5	75.01	6.3	0.080	0.351
CZW-14	75.59	6.9	0.076	0.340
CZW-17.5	71.27	6.1	0.081	0.346
CZW-21	58.72	5.3	0.079	0.384

Fig. 4 shows the temperature distribution at the back surface of modified composites in comparison with pure composite, which was measured experimentally in the first 20 s of the oxyacetylene flame test. At the end of the test, the back surface temperature of a 4 mm thickness CZW-7, CZW-10.5, CZW-14, CZW-17.5, CZW-21 and CZW-0 was recorded in the order given as 115.78, 111.53, 103.12, 102.05, 104.81 and 153.23. It showed that for instant the back surface temperature of CZW-14% was 49% lower than that of the pure composite.

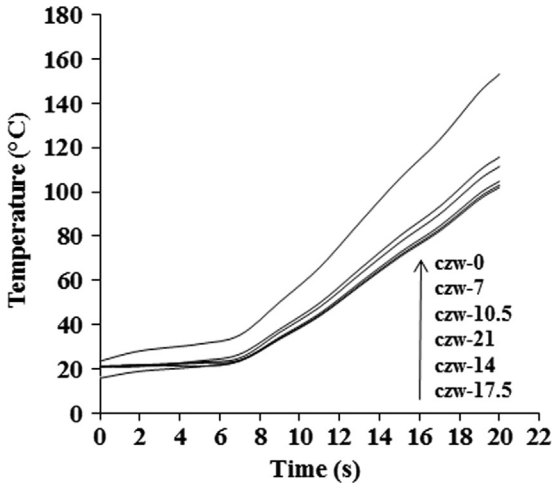

Fig. 4. Temperature distribution of back surface of the as-received composites.

3.4. Structure and surface morphology of char layers

Mass and energy transfer between the material surface and the environment is very complex in the ablation involving a series of chemical and physical reactions. The ablative performance is closely related to the structure, thermal conductivity, and strength of the charred layer and the diffusion rate of pyrolysis gas [24–27,33–35]. Therefore, the difference in ablative properties of different composites is likely caused by the diversity of the char layers formed in the ablation.

Fig. 5 shows the burnt surface of the CZW-0 (Fig. 5a), CZW-7 (Fig. 5b), CZW-14 (Fig. 5c) and back surface of CZW-14 (Fig. 5d) after ablation. The surface color of all the samples which had ZrO_2 changed into pale yellow. In the absence of ZrO_2 and under exposure to the torch, asbestos fibers melted easily into low viscosity, unbounded spheres which rapidly flowed away from the zone touched by the flame plume. A high erosion rate was experienced by the material. Even in a hyperthermal environment characterized by small shear forces, these spheres were easily removed, and left the charred surfaces unprotected. Fig. 5b and c shows the effect of ZrO_2 on ablation of as-received composites. Under exposure to

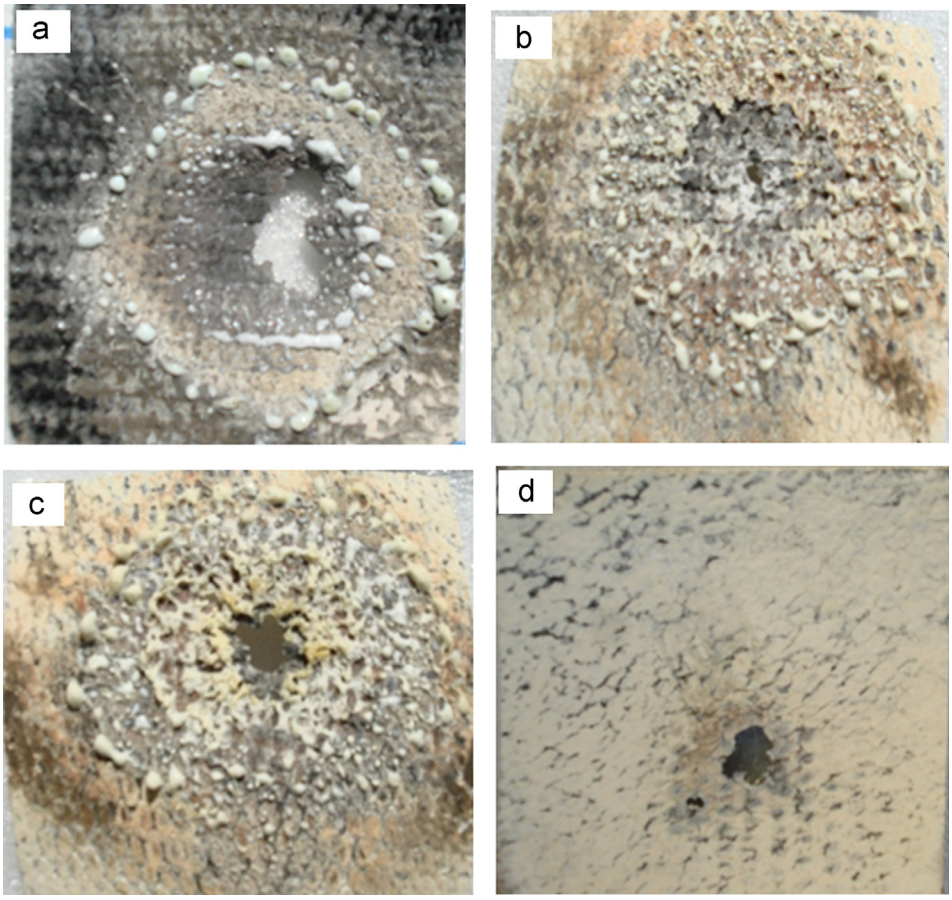

Fig. 5. Digital images of the burnt front surface (a) CZW-0, (b) CZW-7, (c) CZW-14 and (d) the burnt back surface CZW-14 after ablation. (For interpretation of the references to color in this figure legend, the reader is referred to the web version of this article.)

the flame, ZrO_2 melted and produced very high viscosity which slowly flowed away from the zone touched by the flame plume.

On the other hand, the color of the ablated surface changed from black to pale yellow, and yellow, loose ablation layer formed on the surface (especially in samples with ZrO_2 contents of ≥10.5 wt%). The higher ZrO_2 contents were able to effectively freeze the high-viscosity melted ZrO_2 droplets under the zone touched by the flame (Fig. 5b). This condition improved the protection of the charred substrate and the preservation of the surface considerably, leading to a significantly lower erosion rate. Fig. 5d shows the back face of CZW-14 after ablation, as shown by a thin layer of char produced.

SEM study completely confirmed the results of the traditional optical analysis. Increasing the ZrO_2 contents, the erosion rate decreased and the charred substrate increased its capability to freeze the melt droplets under the zone touched

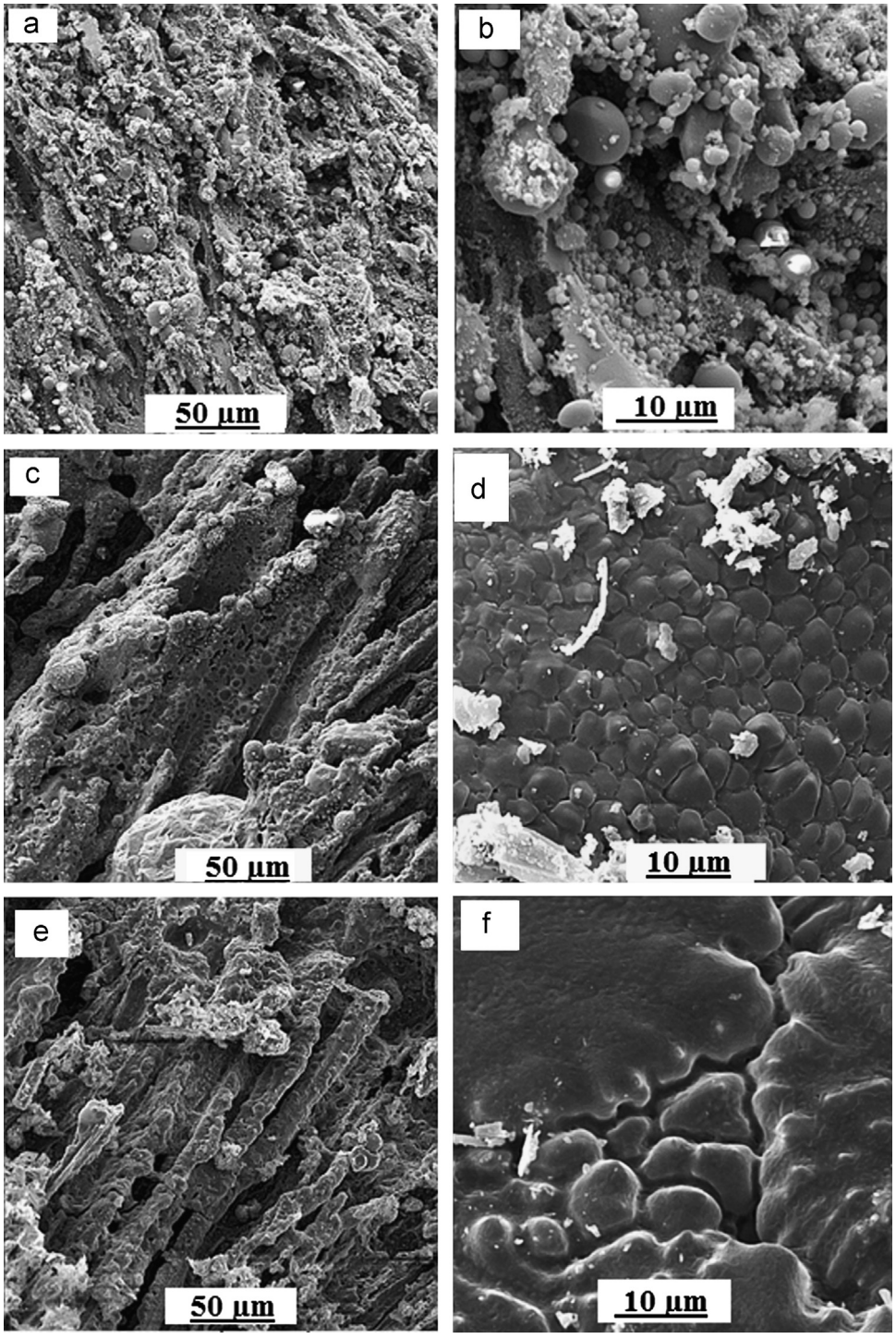

Fig. 6. Ablated surface morphologies of composites (a and b) CZW-0, (c and d) CZW-7 and (e and f) CZW-14.

by the torch, improving the ablation resistance of the as-received composites.

The study of microstructural changes of ablated CZW-0 (Fig. 6a and b) shows the destruction of chrysotile fibers, creation of high porosity, and the residual combustion products which are melted and solidified into spherical shape. These figures show that not only phenolic matrix was sublimated or decomposed completely, but also some asbestos fibers were sublimated as well. This occurred because of the destruction of chrysotile fibers and formation of strips of forsterite and the SiO_2 particles with lower boiling temperature than the flame temperature [14].

The surface morphologies of the modified composites with ZrO_2 after ablation test (Fig. 6c–f) were completely different from that of composite without ZrO_2 (CZW-0). They have much lower porosity than that formed on the surface of CZW-0 and the destruction of fibers is very low (especially in samples with ZrO_2 quantities ≥10.5 wt%). On the other hand, it seems that a thin molten layer covers their surface. This is because ZrO_2, unlike SiO_2, has a high melting point (2800 °C). By melting, ZrO_2 as a highly viscous melt is left on the surface of the composite for it can absorb heat which would be otherwise transferred to the interior of the material. The molten ZrO_2 has high viscosity and strong adhesion to the composite and it partially seals the pores and avoids phenolic matrix and asbestos fibers from more ablation. This is the basic reason for the ablation property improvement of modified composites by ZrO_2 in oxyacetylene torch test.

Char layer which was created in the entire area was exposed to the oxyacetylene flame and then excoriated from the composite surface and made into powder. Phase analysis was carried out by XRD on the composite. Fig. 7 shows the XRD patterns of ZrO_2 modified asbestos fiber composites (CZW-14) before and after ablation. Fig. 8 reveals that the CZW-14 is a composite of monoclinic ZrO_2 and asbestos before ablation. Fig. 7 shows that the char layer of ablated samples consists of mixture of forsterite (Mg_2SiO_4), monoclinic-ZrO_2, cubic-ZrO_2, zirconium carbide (ZrC) and silicon carbide (SiC). This

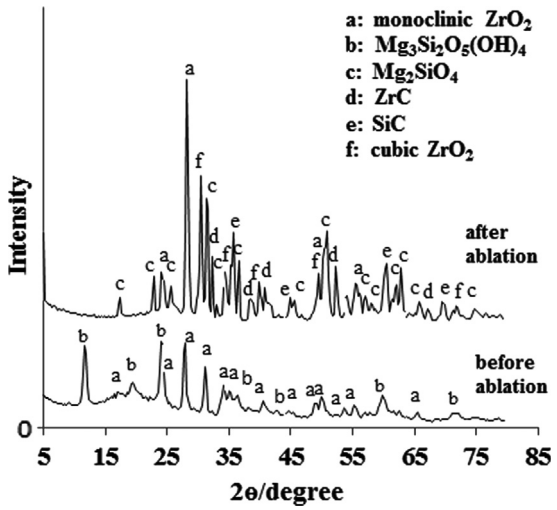

Fig. 7. XRD patterns of CZW-14 before and after ablation.

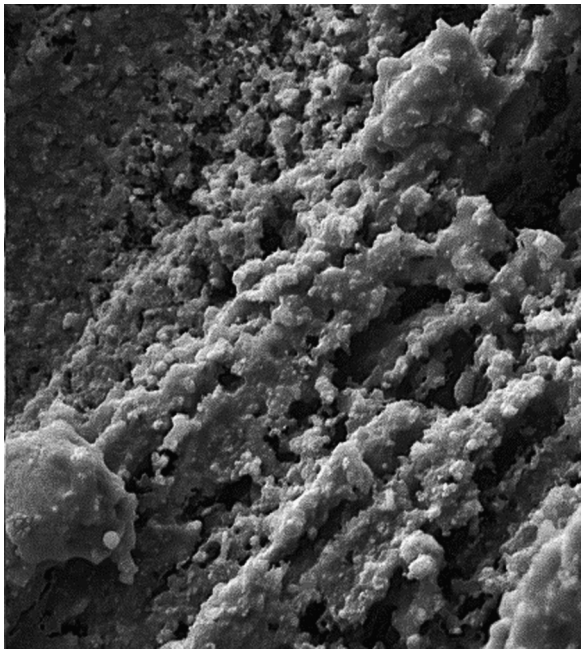

Fig. 8. Morphologies of the tree-coral-like ZrO_2 layer.

indicates that asbestos fibers (chrysotile-type) are destructed completely and converted into forsterite.

As mentioned before, Fig. 5b and c show the pale yellow, loose ablation layer formed on the surface of composites containing ZrO_2 (especially ≥10.5). The microstructure of the pale yellow, loose ablation layer formed on the surface of CZW-21 shows a loose, tree-coral-like ZrO_2 layer without any fiber observed on the surface of the ablation layer (Fig. 8). The relatively large cavities with 5–15 μm diameters were formed because of the burnt-out matrix and the fiber. The surface ablation layer slowed down the heat transfer and gas flow, and therefore it reduced the erosion of materials. After peeling off the loose ZrO_2 layer from the ablation layer, the undersurface layer appeared as an oxidized composite.

3.5. Elemental analysis of char layer

The elemental composition of char layer was characterized by using EDS analysis, the results of which are shown in Fig. 9 and Table 3. On the front surface of the char layer of CZW-0 composite (Fig. 9a), marked as A, the major elements found are: C, O, Mg and Si, in which the last two are relatively low, and in addition to the above elements there are small amounts of Ca and Ir originating from other ingredients which are used in the asbestos fiber. So the white lamellar structures shown by A are mainly composed of C, a result worth noting. The major elements found for marked sector by B (Fig. 9b) are O, Mg and Si and C at relatively low contents. Therefore, the gray spherical structures are mainly composed of O, Mg and Si; implying that the spherical structures on the char layer surface should be made of components that have very high oxygen contents, i.e., forsterite (Mg_2SiO_4). This result was confirmed by Perez-Maqueda et al. [36]. For the char layer of CZW-7 composite, EDS data (Fig. 9c) show that the elements on the

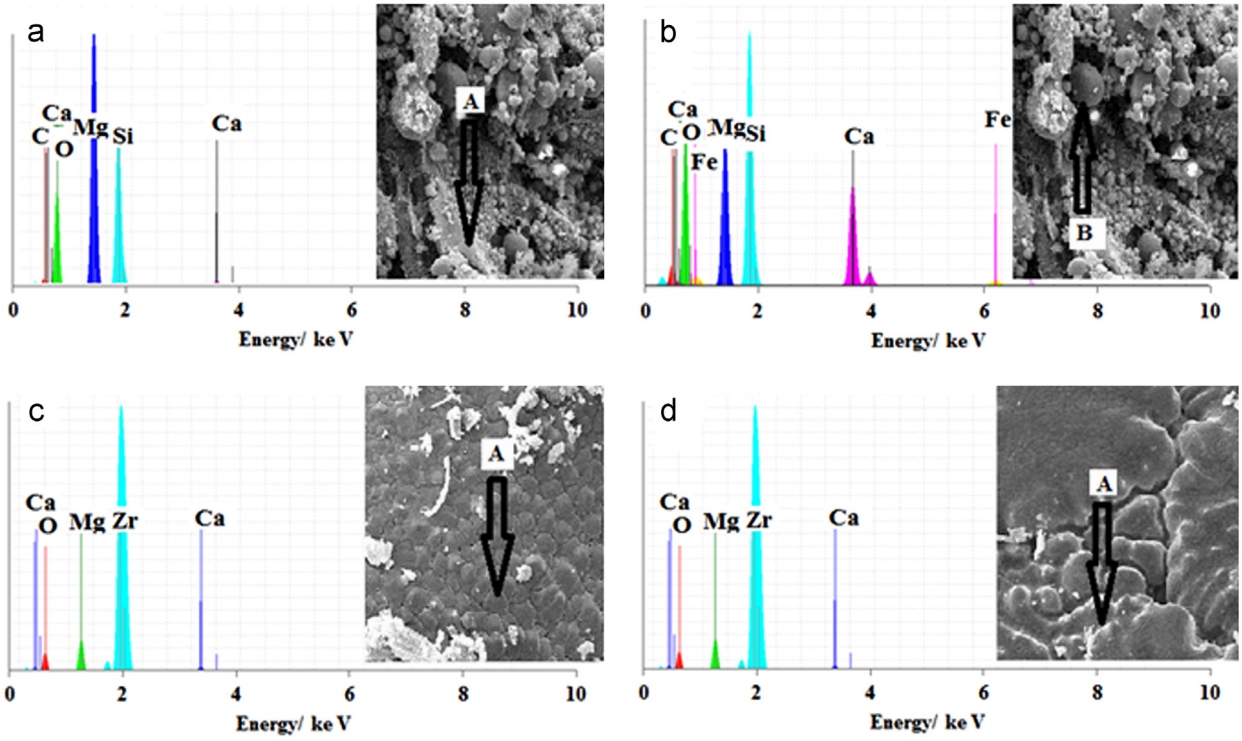

Fig. 9. EDS results of char layers for ablated composites: (a) and (b) CZW-0, (c) CZW-7 and (d) CZW-14.

Table 3
Elemental composition on the front surfaces of char layers for different composites.

Sample	C		O		Si		Mg		Zr		Ca	
	Wt%	At%	Wt%	At%	Wt%	At%	Wt%	At%	Wt%	At%	Wt%	At%
CZW-0												
A	68.29	75.26	27.79	23.00	1.10	0.60	1.91	0.90	–	–	0.29	0.10
B	6.13	9.09	61.79	68.79	19.37	14.19	11.97	7.59	–	–	0.75	0.33
CZW-7												
A	–	–	19.32	55.70	4.29	8.30	–	–	72.34	31.37	4.05	4.63
CZW-14												
A	–	–	18.39	52.75	4.29	8.30	–	–	75.91	38.20	2.32	2.65

front surface are Zr, O and small amounts of Mg and Ca. The data given in Table 2 show that the molar ratio of O to Zr is close to 2:1, which implies that, the thin film layer should be made of ZrO_2. Almost, similar results are observed for the char layer of CZW-14 composite (Fig. 9d). In the modified composites by ZrO_2, the disappearance of the Si element on the center zone of char layer shows that the Si had already vaporized (as SiO_2) in the ablation at temperature over 2000 °C.

3.6. Ablation process and mechanism of the composites

Ablation of polymer composites is a series of complicated chemical reactions (oxidation mainly), the thermal-physical process and mechanical erosion at high-temperatures. There are mainly two kinds of ablation mechanisms including chemical erosion and mechanical denudation. The chemical erosion refers to the oxygen diffusion into the polymer matrix and the heterogeneous reaction of the material with combustion gases. The mechanical denudation means the peeling of the fibers and polymer matrix caused by the shearing forces are due to a flame at high-temperature, high velocity and pressure [37–40]. Observation of the ablation morphology of pure and modified composites (Figs. 5 and 6) is helpful to understand the ablation behavior. The pores, defects and interfaces between the asbestos fibers and phenolic matrix are oxidized initially, so the surface of the specimen becomes loose and perforated. Thus, some passages are formed for oxygen to enter the inner substrate of asbestos/phenolic composites. With the ablation going on, the asbestos fibers and loose phenolic matrix are severely ablated, even washed away by the shearing action of the oxyacetylene flame. As a result, new ablation interface is formed. The asbestos fibers are ablated into pulverulent-shape. During the oxyacetylene torch ablation several degradation processes operate simultaneously. The first one is chemical degradation of composite which involves endothermic pyrolysis of phenolic matrix to char as

shown in Eq. (1).

$$\text{Phenolicmatrix} \rightarrow C(\text{char}) + \quad H_2 + CO + CH_4\text{–heat} \tag{1}$$

In addition to phenolic resin pyrolysis, the following reactions take place:

$$2Mg_3Si_2O_5(OH)_4 \rightarrow 3Mg_2SiO_4 + SiO_2 + 4H_2O \tag{2}$$

$$Mg_2SiO_4 + SiO_2 \rightarrow 2MgSiO_3 \tag{3}$$

$$SiO_2(\text{liquid}) \rightarrow SiO_2(\text{gaseous}) \tag{4}$$

$$ZrO_2(\text{solid}) \rightarrow ZrO_2(\text{liquid}) \tag{5}$$

$$ZrO_2 + 3C(\text{solidchar}) \rightarrow ZrC(\text{solid}) + 2CO(\text{gaseous}) \tag{6}$$

$$SiO_2 + 3C(\text{solidchar}) \rightarrow SiC + 2CO \tag{7}$$

The reactions (2), (3), (6) and (7) may occur in all ablation regions and reactions (4) and (5) only happen at high temperature areas, especially in the surface ablation layer of the composites. When as-received composites are heated in air by oxyacetylene flame first there is the removal of structural OH of chrysotile fiber (reaction 2). After dehydroxylation of chrysotile, forsterite (Mg_2SiO_4) occurs and by increased heating, enstatite ($MgSiO_3$) also appears and the content of forsterite increases as well [41–43]. It is well known that the boiling point of SiO_2 is 2230 °C, while the surface temperature of the char layer is around 3000 °C in the ablation. Therefore, a large amount of SiO_2 evaporates (reaction 4). Under the ablation temperature around 3000 °C, enstatite evaporates incongruently and produces Mg/Si variations in solid (Mg-rich) and gas (Si-rich). These phenomena lead to complete destruction of fibers and they are easily milled to pulverulent-shape material by the shearing force of the flame and the mechanical breakage. This is the main reason for high rate of mass loss for asbestos composites.

Reaction 5 happens in the modified composites with ZrO_2, at high temperature areas. In the case of modified composites, the ablation process may be divided into two steps. At first, the oxidation of phenolic matrix and ablation of fibers begin at low temperature to form spongy structure, and the oxygen diffusion path is formed by the open pores and cracks in the composite. Secondly, ZrO_2 is melted when the char layer temperature is raised around 3000 °C. In the char layer surface high velocity flame made ZrO_2 melt spread out on the ablated surface. The ZrO_2 melt is a thermal barrier with low thermal conductivity. Molten ZrO_2 could reduce heat transfer and oxygen transport to the underlying materials. Therefore, it isolates the heat flux and retards the oxygen to react with the fiber and phenolic matrix. The thermal and ablation properties are thus enhanced. However, when it is cooled down, ZrO_2 is transformed from cubic phase to monoclinic phase, which may lead to its large volume change. ZrO_2 spills off the ablated surface and probably, this is the reason why the tree-coral-like ZrO_2 layer without any fiber is observed upon the surface of the ablation layer (Fig. 8).

As mentioned before, in essence, zirconia-modified composites and SiO_2 produced in composites after oxyacetylene test, are reacting with the charred matrix (6 and 7 reactions), giving ZrC and SiC with the evolution of carbon monoxide gas. Formation of ZrC and SiC are confirmed from XRD studies of ablated surfaces of the as-received composites (Fig. 7).

However, in the outer region, next to the ablated center, ZrO_2 can react with SiO_2 to produce zircon ($ZrSiO_4$) where there is lower temperature, flow rate and pressure relative to the center region. Therefore, ZrO_2 and the produced SiO_2 are sintered together to form a dense layer that block the conducted heat and resist the ultra-high temperature scouring of oxyacetylene flame [44]. Thus, the ablation resistance of the modified composites with ZrO_2 is improved significantly.

4. Conclusion

Asbestos/phenolic composites were prepared by an autoclave curing cycle process. Ablation behavior of the as-produced composites was investigated by oxyacetylene torch test. The thermal stability of asbestos/phenolic composites was improved with the increasing of the ZrO_2 contents. The linear and mass ablation rates for the specimen with a ZrO_2 content of 14 wt% (0.340 mm/s and 0.076 g/s, respectively) decreased by about 58% and 92%, respectively, in comparison with those of pure composites. ZrO_2/asbestos/phenolic composite showed much better ablation resistance than asbestos/phenolic composite because ZrO_2 is melted on the surface and sealed the pores of the composites. On the other hand the melting process of ZrO_2 absorbed the heat that would otherwise transfer to the interior of the material. This greatly improves the ablation property of the asbestos/phenolic composite.

References

[1] G.F. D'Alelio, J.A. Parke, Ablative Plastics, Marcel Dekker, New York, 1971.
[2] E.W. Ungar, Ablation Thermal Protection Systems, Science, New series 158 (1967) 740–744.
[3] C.C. Gary, S.V. Balaji, C. Ioana, Multi-scale simulations of in-depth pyrolysis of charring ablative thermal protection material, Computers and Fluids 45 (2011) 191–196.
[4] J.H. Koo, D.W. Ho, M.C. Bruns, O.A. Ezekoye, A review of numerical and experimental characterization of thermal protection materials—Part II, Properties Characterization, AIAA paper 2007-2131, 2007.
[5] J.H. Koo, D.W. Ho, M.C. Bruns, O.A. Ezekoye, A review of numerical and experimental characterization of thermal protection materials—part III, Experimental Testing, AIAA paper 2007-5773, 2007.
[6] E. Venkatapathy, B. Laub, G.J. Hartman, J.O. Arnold, M.J. Wright, G.A. Allen, Thermal protection system development, testing, and qualification for atmospheric probes and sample return missions examples for saturn, titan and stardust-type sample return, Advances in Space Research 44 (2009) 138–150.
[7] B. Laub, E. Venkatathy, Thermal protection system technology and facility needs for demanding future planetary missions, in: Proceedings of International Workshop on Planetary Probe Atmospheric Entry and Descent Trajectory Analysis and Science, Lisbon, Portugal, 2003.
[8] G. Pulci, F. Fossati, C. Bartuli, T. Valente, Carbon–phenolic ablative materials for re-entry space vehicles, manufacturing and properties, Composites Part A 41 (2010) 1483–1490.
[9] L. Torre, J.M. Kenny, G. Boghetich, A.M. Maffezzoli, Degradation behavior of a composite material for thermal protection systems, Part III

—char characterization, Journal of Materials Science 35 (2000) 4536–4566.
[10] L. Torre, J.M. Kenny, G. Boghetich, A.M. Maffezzoli, Degradation behaviour of a composite material for thermal protection systems, Part I —experimental characterization, Journal of Materials Science 33 (1998) 3137–3143.
[11] W. Zhou, C. Wang, T. Ai, K. Wu, F. Zhao, H. Gu, A novel fiber-reinforced polyethylene composite with added silicon nitride particles for enhanced thermal conductivity, Composites Part A 40 (2009) 830–836.
[12] H. He, R. Fu, Y. Shen, Y. Han, X. Song, Preparation and properties of Si_3N_4/PS composites used for electronic packaging, Composites Science and Technology 67 (2007) 2493–2499.
[13] Z. Guo, T.Y. Kim, K. Lei, T. Pereira, J.G. Sugar, H.T. Hahn, Strengthening and thermal stabilization of polyurethane nanocomposites with silicon carbide nanoparticles by a surface-initiated-polymerization approach, Composites Science and Technology 68 (2008) 164–170.
[14] D. Fang, Z. Chen, Y. Song, Z. Sun, Morphology and microstructure of 2.5 dimension C/SiC composites ablated by oxyacetylene torch, Ceramics International 35 (2009) 1249–1253.
[15] P. Fino, M. Lombardi, G. Malucelli, L. Montanaro, Exploring composites based on PPO blend as ablative thermal protection systems—Part I: the role of layered fillers, Composite Structures 94 (2012) 1067–1074.
[16] P. Fino, M. Lombardi, G. Malucelli, L. Montanaro, Exploring composites based on PPO blend as ablative thermal protection systems—Part II: the role of equiaxial fillers, Composite Structures 94 (2012) 1060–1066.
[17] X. Yang, L. Wei, W. Song, C.Z. hui, Ablative property of ZrC–SiC multilayer coating for PIP–C/SiC composites under oxy-acetylene torch, Ceramics International 38 (2012) 2893–2897.
[18] L. Zhaoqian, L. Hejun, Z. Shouyang, L. Kezhi, Microstructure and ablation behaviors of integer felt reinforced C/C SiC–ZrC composites prepared by a two-step method, Ceramics International 38 (2012) 3419–3425.
[19] S. Xuetao, L. Kezhi, L. Hejun, D. Hongying, C. Weifeng, L. Fengtao, Microstructure and ablation properties of zirconium carbide doped carbon/carbon composites, Carbon 48 (2010) 344–3451.
[20] S.X. Tao, L. Zhi, L.H. Jun, F.Q. Gang, L.S. Ping, D. Fei, The effect of zirconium carbide on ablation of carbon/carbon composites under an oxyacetylene flame, Corrosion Science 53 (2011) 105–112.
[21] C. Zhou, W. Wangping, C. Zhaofeng, C. Xiangna, Q. Jinlian, Microstructural characterization on ZrC doped carbon/carbon composites, Ceramics International 38 (2012) 761–767.
[22] Y. Tong, S. Bai, K. Chen, C/C–ZrC composite prepared by chemical vapor infiltration combined with alloyed reactive melt infiltration, Ceramics International 38 (2012) 5723–5730.
[23] E.L. Corral, L.S. Walker, Improved ablation resistance of C/C composites using zirconium diboride and boron carbide, Journal of the European Ceramic Society 30 (2010) 2357–2364.
[24] A.R. Bahramian, M. Kokabi, M.H. Beheshty, M.H.N. Famili, Thermal degradation process of resole type phenolic matrix/kaolinite layered silicate nanocomposite, Iranian Polymer Journal 16 (2007) 375–387.
[25] A.R. Bahramian, M. Kokabi, M.H. Beheshty, M.H.N. Famili, High temperature ablation of kaolinite layered silicate/phenolic resin/asbestos cloth nanocomposite, Journal of Hazardous Materials 150 (2008) 136–145.
[26] A.R. Bahramian, M. Kokabi, M.H. Beheshty, M.H.N. Famili, Ablation and thermal degradation behaviour of a composite based on resole type phenolic resin: Process modeling and experimental, Polymer 47 (2006) 3661–3673.
[27] A.R. Bahramian, M. Kokabi, Ablation mechanism of polymer layered silicate nanocomposite heat shield, Journal of Hazardous Materials 166 (2009) 445–454.
[28] H.O. Pierson, Handbook of Refractory Carbides and Nitride, Noyes, New Jersey, 1996.
[29] H. Cheng, Z. Chen, J. Tao, B. Yan, C. Li, L. Wang, Y. Zhang, D. Fang, S. Wan, W. Wu, Effect of ZrO_2 powders on the pyrolysis of polycarbosilanes coating under laser ablation, Surface Review and Letters 15 (2008) 469–472.
[30] I. Srikanth, N. Padmavathi, S. Kumar, P. Ghosal, A. Kumar, C.H. Subrahmanyam, Thermal and ablative properties of zirconia, CNT modified carbon/phenolic composites, Composites Science and Technology 80 (2013) 1–7.
[31] M.A. Mirzapour, H. Rezaei, Effect of ZrO_2 on ablation properties of carbon and ceramic fiber composites under oxyacetylene flame, in: Proceedings of the 3rd International Conference on Composites, Characterization, Fabrication and Application, CCFA-3, Tehran, Iran, 2012.
[32] A. Paydayesh, M. Kokabi, A.R. Bahramian, High temperature ablation of highly filled polymer-layered silicate nanocomposites, Journal of Applied Polymer Science 127 (2012) 2776–2785.
[33] L. Torre, J.M. Kenny, G. Boghetich, A. Maffezzoli, Degradation behaviour of a composite material for thermal protection systems Part I char characterization, Journal of Materials Science 33 (1998) 3137–3143.
[34] L. Torre, J.M. Kenny, G. Boghetich, A. Maffezzoli, Degradation behaviour of a composite material for thermal protection systems Part II char characterization, Journal of Materials Science 35 (1998) 3145–3149.
[35] L. Torre, J.M. Kenny, G. Boghetich, A. Maffezzoli, Degradation behaviour of a composite material for thermal protection systems Part III char characterization, Journal of Materials Science 35 (1998) 4563–4566.
[36] L.A.P. Maqueda, V. Balek, J. Poyato, J. Subrt, M. Benes, V.R. Valle, I.M. Buntseva, I.N. Beckman, J.L.P. Rodriguez, Transport properties and microstructure changes of talc characterized by emanation thermal analysis, Journal of Thermal Analysis and Calorimetry 92 (2008) 253–258.
[37] J.M. Su, Research and application of bulk-needled-felt reinforced carbon composites throat, New Carbon Materials 12 (1997) 46–49.
[38] H. Cui, J.M. Su, R.Z. Li, H.J. Li, M.K. Kang, On improving anti ablation property of multi-matrix C/C to withstand 3700 K, Journal of Northwestern Polytechnic University 18 (2000) 669–673.
[39] J. Yin, X. Xiong, H.B. Zhang, B.Y. Huang, Microstructure and ablation performances of dual-matrix carbon/carbon composites, Carbon 44 (2006) 1690–1694.
[40] C.Y. Li, K.Z. Li, H.B. Ouyang, H.J. Li, Ablation behavior of HfC modified carbon/carbon composites, Rare Metal Materials and Engineering 35 (2006) 365–368.
[41] T. Zaremba, A. Krzakala, J. Piotrowski, D. Garczorz, Study on the thermal decomposition of chrysotile asbestos, Journal of Thermal Analysis and Calorimetry 101 (2010) 479–485.
[42] A.F. Gualtieria, A. Tartagliab, Thermal decomposition of asbestos and recycling in traditional, Journal of the European Ceramic Society 20 (2000) 1409–1418.
[43] F. Dellisanti, V. Minguzzi, N. Morandi, Experimental results from thermal treatment of asbestos containing materials, GeoActa 1 (2002) 61–70.
[44] Q.M. Liu, L.T. Zhang, J. Liu, X.G. Luan, L.F. Cheng, Y.G. Wang, The oxidation behavior of SiC–ZrC–SiC coated C/SiC minicomposites at ultrahigh temperatures, Journal of the American Ceramic Society 93 (2010) 3990–3992.